Disorder-assisted graph coloring on quantum annealers

Andrzej Więckowski [1], Sebastian Deffner [2] and Bartłomiej Gardas [3,4]

[1] *Department of Theoretical Physics, Faculty of Fundamental Problems of Technology, Wrocław University of Science and Technology, 50-370 Wrocław, Poland*

[2] *Department of Physics, University of Maryland, Baltimore County, Baltimore, Maryland 21250, USA*

[3] *Institute of Theoretical and Applied Informatics, Polish Academy of Sciences, Bałtycka 5, 44-100 Gliwice, Poland*

[4] *Jagiellonian University, Marian Smoluchowski Institute of Physics, Łojasiewicza 11, 30-348 Kraków, Poland*

(Received 5 June 2019; published 3 December 2019)

We are at the verge of a new era, which will be dominated by noisy intermediate-scale quantum devices. Prototypical examples for these new technologies are present-day quantum annealers. In the present work, we investigate to what extent static disorder generated by an external source of noise does not have to be detrimental, but can actually assist quantum annealers in achieving better performance. In particular, we analyze the graph coloring problem that can be solved on a sparse topology (i.e., chimera graph) via suitable embedding. We show that specifically tailored disorder can enhance the fidelity of the annealing process and thus increase the overall performance of the annealer.

DOI: 10.1103/PhysRevA.100.062304

I. INTRODUCTION

The first concept of quantum computing was formulated several decades ago in an attempt to faithfully simulate many-body quantum systems, which remains conjectured to be an impossible feat with classical computers [1,2]. However, only very recently novel technologies have become available that promise to make quantum computers a practical reality [3]. Quite remarkably, already the first generation of fully operational quantum computers is expected to outperform (for specific tasks) even the most advanced, state-of-the-art classical computers [3,4]. To be ready for the first physical realizations of such powerful information technology, quantum computer science has been developing a plethora of quantum algorithms for a wide variety of optimization problems [5]. Famous examples include the Deutsch-Jozsa algorithm [6] to evaluate a function, the Grover algorithm [7] for searches of a (possibly large) database, or Shor's algorithm [8] designed for prime factorization.

In the present work we will focus on adiabatic quantum computation (AQC) [9], which relies on quantum annealing [10]. In comparison to other computational paradigms, AQC is technologically slightly more advanced due to the commercial availability of D-Wave's quantum annealers [11–13]. Adiabatic quantum computing is a computational paradigm [14] that has the potential to solve many problems that a universal quantum computer can also solve [15]. Although a polynomial time penalty may be necessary to achieve this, AQC promises to outperform classical computers in many practical cases [16].

AQC relies on the quantum adiabatic theorem [9]. In this paradigm, a quantum system is prepared in the ground state of an initial ("easy") Hamiltonian H_i. Then, the system is let to evolve adiabatically—infinitely slowly—towards the ground state of the final Hamiltonian H_f. The latter system encodes the problem of interest and its ground state stores the desired solution (i.e., an answer to the problem). Devices that can realize such evolution are called quantum annealers [10]. Quantum annealers are typically designed with one and only one particular task in mind—namely, to solve combinatorial optimization problems from the **NP** complexity class [17,18]. These problems are "very hard" to solve with classical computers; however, their solutions can still be verified (in polynomial time).

Scaling advantages of quantum annealing over classical annealing have been identified [19]. However, currently available technology still exhibits hardware issues, of which the most important one is static disorder [20–24]. Rather counterintuitively, however, it also has been shown that static disorder is not always detrimental, but can rather be a valuable resource in achieving quantum tasks [25,26].

In the present work, we study the influence of static disorder on the annealing dynamics and analyze its effect on the performance of near-term quantum annealers. To this end, we mainly focus on a selected problem of graph coloring [27]. This is a fundamental problem in modern computer science with various applications in many different areas, e.g., in scheduling [28], pattern [29], and frequency [30] matching, or memory allocation [31], to name just a few.

The main objective of the graph coloring problem is to find a minimal number of colors, *chromatic number*—$\chi(G)$, that are required to color a graph G, so that no adjacent sites share the same color. In this context, colors can encode any arbitrary information. Typical examples are shown in Fig. 1. Based on numerical analysis of relatively small system sizes, we suggest that for the graph coloring problem D-Wave-like annealers may actually be robust against certain types of noise. Even more importantly, we will see that particular types of disorder can assist the adiabatic computation to achieve better performance.

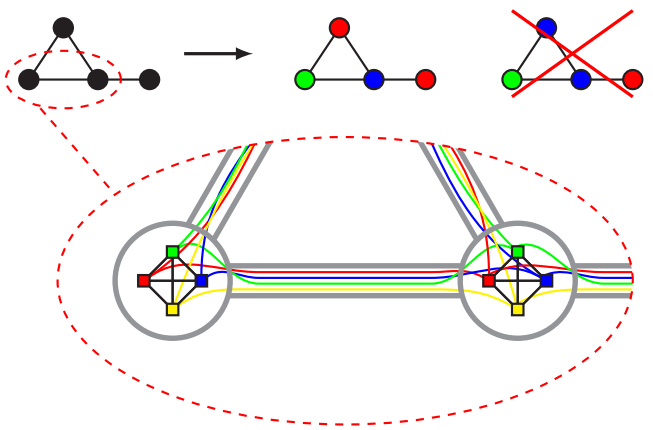

FIG. 1. Graph coloring problem exemplified with $N = 4$ vertices and $K = 3$ colors. A different color is assigned to adjacent vertices. Other configurations are *not* valid solutions. A binary variable $X_{ic} = 1$ represents a vertex $i \leqslant N$ having a color $c \in \{1, 2, \ldots, K\}$. Otherwise, we set $X_{ic} = 0$; cf. Eq. (3).

II. DISORDER GRAPH COLORING PROBLEM

The dynamics of quantum annealers is typically described by the following Hamiltonian,

$$\hat{H}(s) = f(s)\hat{H}_{\rm i} + [1 - f(s)]\hat{H}_{\rm f}, \quad s \in [-1, 1], \tag{1}$$

where $f(s) \in [0, 1]$ could be an arbitrary function such that $f(-1) = 1$ and $f(1) = 0$ [32]. Typically, $f(s) = s + 1$, where $s(t) = t/\tau$ and τ is the annealing time [23]. For the present purposes, initial and final Hamiltonian are instances of the Ising spin glass [10], where, in particular,

$$\hat{H}_{\rm f} = \sum_{\langle i,j\rangle\in\mathcal{E}} J_{ij} S_i^z S_j^z + \sum_{i\in\mathcal{V}} h_i S_i^z, \quad \hat{H}_{\rm i} = 4\sum_{i\in\mathcal{V}} S_i^x. \tag{2}$$

Here, the problem Hamiltonian, $\hat{H}_{\rm f}$, is defined on a graph, $\mathcal{G} = (\mathcal{E}, \mathcal{V})$, specified by its edges, $\mathcal{E}$, and vertices, $\mathcal{V}$. This simple model can already be realized with present-day quantum annealers [19], where the graph $\mathcal{G}$ is set to reflect the chimera [33,34] or pegasus topology [35,36]. The programmable input parameters [37] are the elements of the coupling matrix, J_{ij}, and the on-site magnetic fields, h_i. Spin operators are denoted by S_i^z, S_i^x and they describe spins in the z, x directions, respectively.

All Ising variables can admit only two values ($s_i = \pm 1$). Since there are, however, typically more than two colors necessary to solve a graph coloring problem, one cannot map it *directly* onto the Ising Hamiltonian. Thus graph coloring problems are first expressed as spin lattices, where the spins can take more than two values. These so-called Potts models [38,39] can then be mapped onto the Ising Hamiltonian using a suitable embedding (i.e., with the help of auxiliary variables).

When designing quantum algorithms, it is often convenient to work with the quadratic unconstrained binary optimization framework or QUBO [40]. Here, we introduce a binary variable $X_{ic} = 1$ if a vertex $i \in \{1, 2, \ldots, N\}$ is colored with a color $c \in \{1, 2, \ldots, K\}$ and we set $X_{ic} = 0$ otherwise. Then the graph coloring problem can be formulated in the following simple terms (cf. Fig. 1):

$$\hat{H}_{\rm f}^{\rm Q} = \sum_{i=1}^{N}\left(1 - \sum_{c=1}^{K} X_{ic}\right)^2 + \sum_{\langle i,j\rangle}\sum_{c=1}^{K} X_{ic}X_{jc}, \tag{3}$$

where $\langle i, j\rangle$ indicates summation over all connected vertices. If the ground state of the Hamiltonian in Eq. (3), corresponding to the energy $E = 0$, exists then the graph G can be properly colored with at least K colors. The purpose of the first term in the above Hamiltonian is to assure that each vertex i is colored with only one specific color c, as only then $\sum_{c=1}^{K} X_{ic} = 1$. The second term introduces an energy penalty whenever neighboring vertices have the same color c. Similar encoding strategies have also been discussed in the context of quantum error correcting codes for quantum annealers [41].

Having formulated the graph coloring problem in terms of binary variables, one can convert it back into the Ising Hamiltonian, which is more common for quantum annealers. Namely,

$$\hat{H}_{\rm f}^{\rm I} = \sum_{i=1}^{N} J_{ii} \sum_{c_1<c_2} S_{ic_1}^z S_{ic_2}^z + \sum_{\langle i,j\rangle} J_{ij} \sum_{c=1}^{K} S_{ic}^z S_{jc}^z + \sum_{i=1}^{N} h_i \sum_{c=1}^{K} S_{ic}^z + C, \tag{4}$$

where $S_{ic}^z = X_{ic} - 1/2$ is the spin z operator indexed by two variables (i, c); $C = [1 + K(K - 3)/4]N + K|E|/4$ is a constant and $|E|$ denotes the total number of edges. The coefficients h_i are given by

$$h_i = K + \frac{1}{2}\deg(i) - 2, \quad J_{ij} = \begin{cases} 2, & i = j, \\ 1, & i \neq j, \end{cases} \tag{5}$$

where $\deg(i)$ is the number of edges at vertex i.

Current quantum annealers, such as the D-Wave machine, are imperfect due to a variety of factors, chief among them is *static disorder* originating in the limited control at the hardware level [20,42–47]. Therefore, our objective is to investigate what happens to the quantum annealing when all couplings J_{ij} and magnetic fields h_i are slightly perturbed. To be more specific, we introduce static disorder,

$$h_i \to h_i + \delta h_i, \quad J_{ij} \to J_{ij} + \delta J_{ij}, \tag{6}$$

where perturbations δh_i and δJ_{ij} are random variables with flat distributions and symmetric amplitudes, e.g., $\delta J_{ij} \in [-W_J, W_J]$ and $\delta h_i \in [-W_h, W_h]$ [48].

For the sake of simplicity and without any loss of generality we focus in particular on the disorder generator where $\delta J_{ij} = 0$ and moreover

$$h_i \to \begin{cases} h_i + \delta h_i, & \text{for } h_i + \delta h_i < \max\{h_i\}, \\ \max\{h_i\}, & \text{otherwise.} \end{cases} \tag{7}$$

Such disorder (6) mimics to some extent a situation in which the actual values of interaction strengths at the hardware level differ from the input parameters provided by the programmer operating at the software level.

It is important to emphasize that not any kind of disorder is beneficial for quantum annealing. Rather, we will show in the present work that some specific disorder can assist in

dynamically separating the ground state out of the energy spectrum, and thus protecting the ground state against parasitic excitations.

III. RESULTS

To investigate the dynamics and annealing of the graph coloring problem formulated in Eq. (4), we focus on all nonisomorphic graphs, $G(E, V)$, having $|V| = 3, 4, 5$ vertices and for which the chromatic number $\chi(G) = K > 2$ [49]. We omit the $K = 2$ case as one can reduce its problem Hamiltonian to the antiferromagnetic Ising model.

The quality of a quantum computation and annealing can be measured in various ways [50]. For instance, one may try to count defects [23], estimate fluctuations [24], calculate the fidelity between the final state, $|\psi(\tau)\rangle$, and the true ground state of the problem Hamiltonian [51], $|\phi\rangle$, or simply determine the difference between their corresponding energies, $\delta E = \langle\psi(\tau)|\hat{H}|\psi(\tau)\rangle - \langle\phi|\hat{H}|\phi\rangle$ [21].

In the present work we calculate the probability to observe the correct final result,

$$P = \sum_{i\in\mathcal{S}} |\langle\psi(\tau)|\phi_i\rangle|^2. \tag{8}$$

Here, $\mathcal{S}$ is a set that labels all possible solutions, $|\phi_i\rangle$, of the disorder-free problem encoded in the Hamiltonian (4). The final state $|\psi(\tau)\rangle$ is obtained by solving the time-dependent Schrödinger equation, $i\partial_t|\psi(t)\rangle = \hat{H}(t)|\psi(t)\rangle$, numerically [52,53]. The total Hamiltonian $\hat{H}(t)$ is defined in Eq. (1) with the objective Hamiltonian (encoding the graph coloring problem) given by Eq. (4) where all couplings, J_{ij}, and biases, h_i, are redefined according to Eq. (6).

A priori, the disorder amplitudes W_h, W_J could be arbitrarily large. However, to ensure that the ground state of the disordered problem matches at least one solution to the disorder-free problem at all, both W_h, W_J need to be carefully chosen. For instance, picking $W_J = W_h = 0.5$ guarantees 0.99 probability of this event to occur (cf. Fig. 2). For the sake of simplicity, we choose a simple annealing protocol such that $f(t) = t/\tau$. Moreover, we assume without loss of generality that $W_J \equiv 0$.

A. Disordered energy spectrum

As depicted in Fig. 3, introducing the disorder to the Hamiltonian (4) removes the degeneracy of its ground state. As a result, a solution to the graph coloring problem can be found not only in the degenerate ground state (as in the disorder-free case) but also in low-energy spectrum consisting of $M \ll 2^{KN}$ states. In principle, this effect has the potential to increase the overall chances of finding a correct solution, in particular close to the adiabatic limit, e.g., on a time scale $\tau \sim 1/\Delta$. Here, $\Delta := E_{i_0} - E_0$ is an effective gap, that is, the difference between the ground-state energy E_0 and the energy of the first *accessible* state, E_{i_0}, which does *not* encode a solution.

B. Disorder-assisted dynamics

In Fig. 4 we depict the probability to find the correct answer (8) as a function of the annealing time τ for the disordered and disorder-free systems. In the adiabatic limit where $\tau \gg 1/\Delta$, the disorder-free system is more likely to reach the ground state than the disordered one. Nevertheless, introducing disorder into the system does *not* significantly affect the final probability.

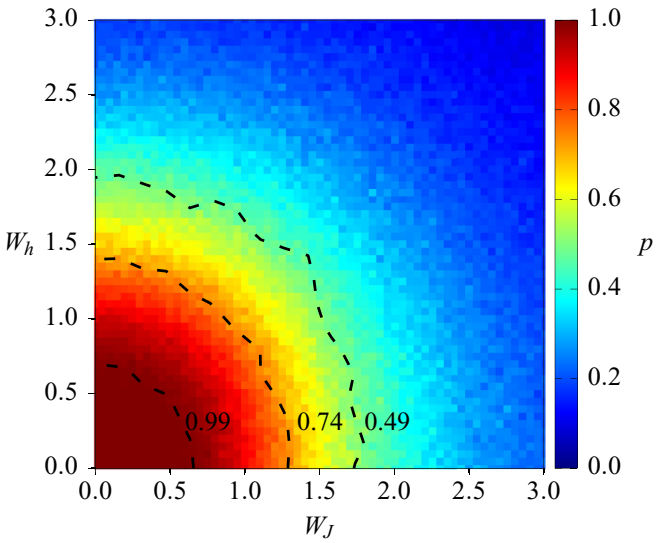

FIG. 2. Influence of the disorder's amplitudes (W_h, W_J) on the ground-state properties of the system's Hamiltonian (2). Here, p is the probability for the ground state of the disordered system being any of the solutions to the disorder-free problem [cf. Eq. (6)]. Contours show probabilities 0.99, 0.74, and 0.49, respectively. The result has been obtained for the triangle topology ($|V| = 3$).

Figure 4 also shows "optimal" results (black dashed lines), obtained as follows: (*i*) for the best found configuration, h_i^{opt}, for the disorder system, i.e., with the biggest probability P, we add a normal noise to h_i^{opt} with zero mean and unit variance multiplied by the factor $\eta = 0.1$; (*ii*) we then repeat the simulations for different realizations of the noise; (*iii*) finally, we average over all realizations.

In Figs. 5(a) and 5(b) we compare a generic [Eq. (6)] and specific [Eq. (7)] type of disorder for different typologies by analyzing the density $\rho(P)$ of a random variable P. As one can see, the density corresponding to Eq. (7) is much "narrower." Furthermore, its mean value is larger than the mean value corresponding to the density for the disorder-free case.

On the other hand, for small and moderate τ we observe that the probability to find the correct solutions is typically larger for the disordered Hamiltonian than in the disorder-free situation. Thus it is not far-fetched to realize that one can always try to find τ_0 such that $P_{\text{free}}(\tau_0) < P_{\text{disorder}}(\tau_0)$. This suggests a different strategy to perform computation with noisy near-term quantum annealers. Rather then trying to operate the annealer as adiabatically as possible, one identifies the "sweet spot," τ_0, at which the quantum annealer has optimal performance, even better than in the ideal, disorder free case, despite the inevitable noise in the system. For instance, Fig. 5(c) indicates a clear maximum. Quite remarkably, we also notice that this is truly a finite-time effect. In Fig. 5(d) we plot the optimal value of the noise amplitude as a function of the anneal time. We observe that in the adiabatic limit the disorder-free case is the only "good" realization.

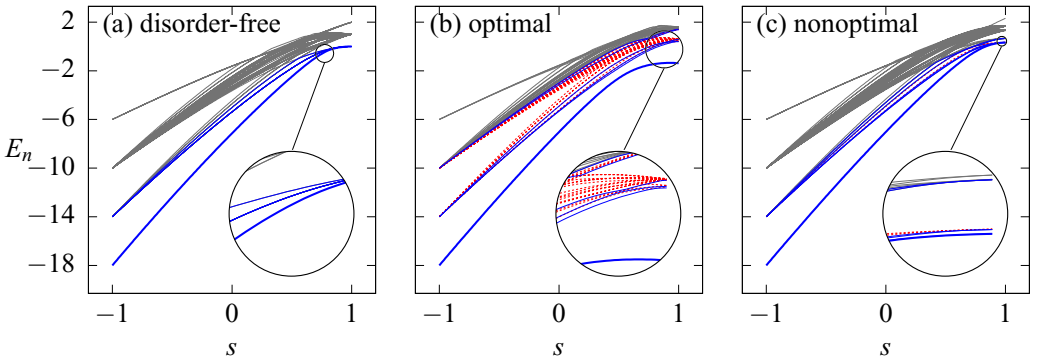

FIG. 3. Structure of the low-energy spectrum for the disorder-free (a) and disordered Hamiltonians [(b), (c)]; cf. Eq. (1). The ground state, $E_n(s = 1)$, is degenerate for the disorder-free case and thus encodes all different solutions (marked here as blue solid lines) to the graph coloring problem. The degeneracy is then removed when disorder is incorporated into the system; cf. Eq. (7). Optimally, both the ground state and also excited states encode correct solutions with no "impurities" in between (i.e., low-energy states representing *incorrect* solutions—marked as red dashed lines). This situation increases the effective gap, Δ (defined as the difference between the ground state and the first accessible state), decreasing the computational and annealing time, τ; cf. Fig. 4. In contrast, nonoptimal realizations result in impurities causing the effective gap to shrink. This leads to an increase of the annealing time τ. All plots has been obtained for the triangle topology.

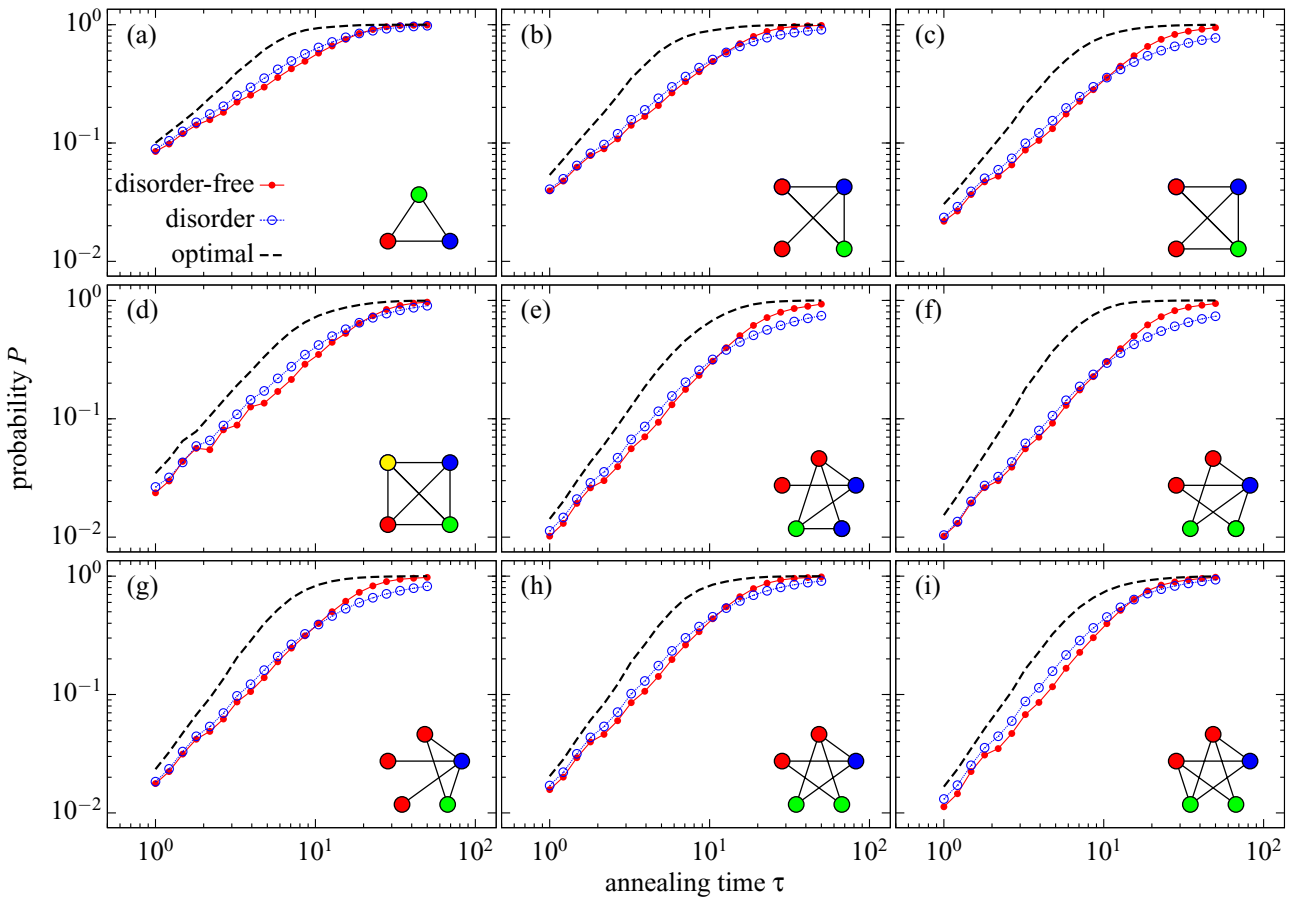

FIG. 4. Probability P to observe the correct final result defined in Eq. (8) as a function of the computational and annealing time, τ, for selected problem typologies. Red solid lines correspond to the disorder-free case, e.g., $W_h = W_J = 0$, whereas blue dashed lines depict results for the disordered case, where magnetic fields are perturbed according to Eq. (7) with $W_h = 1$. Here, $f(t) = t/\tau$. The corresponding low-energy spectra for all three cases are depicted in Fig. 3. Black dashed line corresponds to the optimal disorder realization—which is obtained by averaging all realizations with additional normal noise with zero mean and unit variance multiplied by the factor $\eta = 0.1$ (added to the best found configuration h_i^{opt} for the disorder system)—cf. Fig. 3(b).

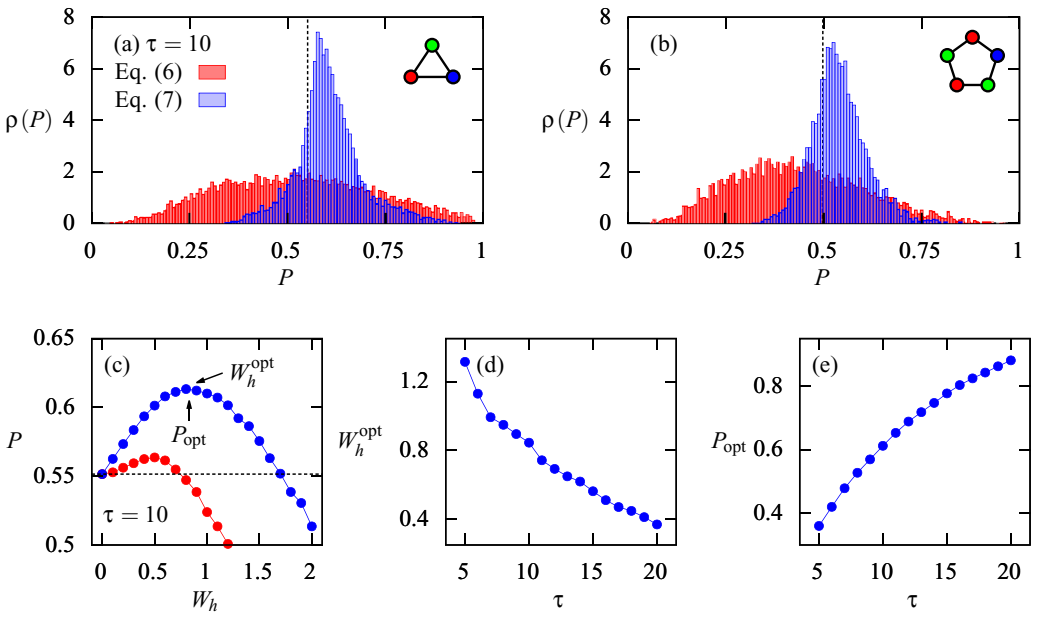

FIG. 5. (a), (b) Comparison between a generic [Eq. (6)] and specific [Eq. (7)] type of disorder for different typologies ($\tau = 10$, $W_h = 1$, and $W_J = 0$). Here, $\rho(P)$ denotes the density of random variable P defined in Eq. (8). (c) Influence of the disorder amplitude W_h on probability P. Result for disorder-free case is marked with black dashed line. (d), (e) Annealing time τ dependence of optimal values W_h^{opt} and P_{opt}. The result in (a), (c)–(e), and (b) has been obtained for the triangle and pentagon topologies, respectively; $W_J = 0$.

However, the impact of the disorder on the success probability is still relatively small. This is illustrated Fig. 5(e). Even at optimal noise strength P is significantly larger for slower processes. Thus we must ask whether the noise can be modified to make it more "useful."

C. Optimizing disorder

Note that so far we have assumed that noise in the qubit-qubit couplings is uniformly distributed. However, we have also already realized that at intermediate anneal times the presence of noise actually assists the quantum annealer in finding the correct solution. The natural question then is whether the disorder in the system can be engineered to further enhance this effect—in other words, how to modify the distribution of the noise in our favor. It is then instructive to analyze the energy diagram and dynamics of single realizations of the disordered problem.

To this end, inspect again Fig. 3. We observe that in the disorder-free case due to the presence of the degeneracy in the ground state the effective gap Δ never actually closes; cf. Fig. 3(a). The same holds true for "good" realizations, except that the effective gap opens even wider due to the lack of degeneracy; compare Fig. 3(b). On the contrary, for all the cases we identify as "bad," we see some mixture of correct and incorrect solutions that basically behave like impurities causing the effective gap to shrink [cf. Fig. 3(c)]. Thus removing those impurities increases the effective gap which causes the adiabatic threshold to decrease.

Thus minimizing the influence of the remaining, "bad" realizations may decrease the total time necessary to find a correct solution substantially. This is also demonstrated in Fig. 4 where the average dynamics is computed over only those realizations that correlate with correct solutions. This clearly demonstrates the advantage of disordered dynamics over the "ideal," disorder-free situation.

IV. CONCLUSIONS

It is still a commonly accepted creed that noise and disorder in computing hardware have exclusively negative consequences. In the present work, we have shown that this is not always the case and that static disorder can actually assist quantum annealers in successfully performing their tasks. More specifically, we have studied the graph coloring problem [21] on disorder-free and disordered quantum annealers.

On a fundamental level, our results clearly exhibit that moderate noise in the qubit-qubit couplings does not only *not* deter the annealer from finding the correct solution, but also that there are instances where disorder assists the annealer to perform in *finite time*. A more thorough analysis revealed that in truly adiabatic operation, i.e., for very large anneal times, noise is, indeed, detrimental. However, we also found that for short anneal times static disorder can be tuned to significantly enhance the performance of the quantum annealer.

Interestingly, recently a new massively parallel algorithm for simulated annealing has been proposed [54]. This method contains a nondeterministic element—lack of synchronization between CUDA threads, which could be (re)interpreted as a source of noise.

On a more practical note, our results may suggest an answer to a conundrum about existing hardware. Systems like the D-Wave machine are known to be subject to electrode noise, which can lead to severe disorder in the on-site fields and qubit couplings. Nevertheless, in particular graph coloring problems have been shown to be solved rather accurately [55–57]. A conjecture that can be drawn now is that the

D-Wave machine may be operating exactly in such a disorder-assisted regime.

Of course, further characterization of the D-Wave machine appears necessary to verify our hypothesis. However, if this is indeed the case, then the performance of the machine could be dramatically enhanced by postselecting the answers on the noise distribution (which will need to be measured independently).

We end on a more speculative note: in the present work, we have seen that disorder can be beneficial in small to moderate-sized problems. We are reasonably optimistic that this observation is generic, and that it will also survive in large scale problems. However, only future research will tell whether this is indeed the case.

ACKNOWLEDGMENTS

We thank Marcin Mierzejewski and Konrad Jałowiecki for fruitful discussions. This work was supported by the National Science Centre, Poland under Projects No. 2016/23/B/ST3/00647 (A.W.) and No. 2016/20/S/ST2/00152 (B.G.). S.D. acknowledges support from the US National Science Foundation under Grant No. CHE-1648973.

[1] R. P. Feynman, There's plenty of room at the bottom, J. Microelectromechanical Syst. **1**, 60 (1992).
[2] R. P. Feynman, Simulating physics with computers, Int. J. Theor. Phys. **21**, 467 (1982).
[3] B. C. Sanders, *How to Build a Quantum Computer* (IOP Publishing, Bristol, 2017), p. 2399.
[4] F. Sheldon, F. L. Traversa, and M. D. Ventra, Taming a non-convex landscape with dynamical long-range order: memcomputing the Ising benchmarks, Phys. Rev. E **100**, 053311 (2019).
[5] M. Mosca, Quantum algorithms, arXiv:0808.0369.
[6] D. Deutsch and R. Jozsa, Rapid solution of problems by quantum computation, Proc. R. Soc. London A **439**, 553 (1992).
[7] L. K. Grover, Quantum Mechanics Helps in Searching for a Needle in a Haystack, Phys. Rev. Lett. **79**, 325 (1997).
[8] P. Shor, Polynomial-time algorithms for prime factorization and discrete logarithms on a quantum computer, SIAM J. Sci. Stat. Comput. **26**, 1484 (1997).
[9] E. Farhi, J. Goldstone, S. Gutmann, and M. Sipser, Quantum computation by adiabatic evolution, arXiv:quant-ph/0001106v1.
[10] T. Kadowaki and H. Nishimori, Quantum annealing in the transverse Ising model, Phys. Rev. E **58**, 5355 (1998).
[11] R. Harris, M. W. Johnson, T. Lanting, A. J. Berkley, J. Johansson, P. Bunyk, E. Tolkacheva, E. Ladizinsky, N. Ladizinsky, T. Oh *et al.*, Experimental investigation of an eight-qubit unit cell in a superconducting optimization processor, Phys. Rev. B **82**, 024511 (2010).
[12] M. W. Johnson, M. H. Amin, S. Gildert, T. Lanting, F. Hamze, N. Dickson, R. Harris, A. J. Berkley, J. Johansson, P. Bunyk *et al.*, Quantum annealing with manufactured spins, Nature (London) **473**, 194 (2011).
[13] S. Boixo, T. Albash, F. M. Spedalieri, N. Chancellor, and D. A. Lidar, Experimental signature of programmable quantum annealing, Nat. Commun. **4**, 2067 (2013).
[14] T. Albash and D. A. Lidar, Adiabatic quantum computation, Rev. Mod. Phys. **90**, 015002 (2018).
[15] D. Aharonov, W. van Dam, J. Kempe, Z. Landau, S. Lloyd, and O. Regev, Adiabatic quantum computation is equivalent to standard quantum computation, SIAM Rev. **50**, 755 (2008).
[16] E. Farhi, J. Goldstone, S. Gutmann, J. Lapan, A. Lundgren, and D. Preda, A quantum adiabatic evolution algorithm applied to random instances of an NP-complete problem, Science **292**, 472 (2001).
[17] F. Barahona, On the computational complexity of Ising spin glass models, J. Phys. A: Math. Gen. **15**, 3241 (1982).
[18] J. D. Biamonte and P. J. Love, Realizable Hamiltonians for universal adiabatic quantum computers, Phys. Rev. A **78**, 012352 (2008).
[19] T. Albash and D. A. Lidar, Demonstration of a Scaling Advantage for a Quantum Annealer over Simulated Annealing, Phys. Rev. X **8**, 031016 (2018).
[20] J. Brugger, C. Seidel, M. Streif, F. A. Wudarski, and A. Buchleitner, Quantum annealing in the presence of disorder, arXiv:1808.06817v2.
[21] K. Kudo, Constrained quantum annealing of graph coloring, Phys. Rev. A **98**, 022301 (2018).
[22] K. Kudo, Localization in the constrained quantum annealing of graph coloring, arXiv:1902.07888.
[23] B. Gardas, J. Dziarmaga, W. H. Zurek, and M. Zwolak, Defects in quantum computers, Sci. Rep. **8**, 4539 (2018).
[24] B. Gardas and S. Deffner, Quantum fluctuation theorem for error diagnostics in quantum annealers, Sci. Rep. **8**, 17191 (2018).
[25] L. Novo, M. Mohseni, and Y. Omar, Disorder-assisted quantum transport in suboptimal decoherence regimes, Sci. Rep. **6**, 18142 (2016).
[26] G. M. A. Almeida, F. A. B. F. de Moura, T. J. G. Apollaro, and M. L. Lyra, Disorder-assisted distribution of entanglement in *xy* spin chains, Phys. Rev. A **96**, 032315 (2017).
[27] P. Formanowicz and K. Tanaś, A survey of graph coloring - its types, methods and applications, Found. Comput. Decision Sci. **37**, 223 (2012).
[28] D. Marx, Graph colouring problems and their applications in scheduling, Period. Polytech. Electr. Eng. **48**, 11 (2004).
[29] H. B. Silva, P. Brito, and J. P. da Costa, A partitional clustering algorithm validated by a clustering tendency index based on graph theory, Pattern Recognit. **39**, 776 (2006).
[30] T. Park and C. Y. Lee, Application of the graph coloring algorithm to the frequency assignment problem, J. Oper. Res. Soc. Jpn. **39**, 258 (1996).
[31] G. J. Chaitin, Register allocation & spilling via graph coloring. SIGPLAN Not. **17**, 98 (1982).
[32] T. Lanting, A. J. Przybysz, A. Y. Smirnov, F. M. Spedalieri, M. H. Amin, A. J. Berkley, R. Harris, F. Altomare, S. Boixo, P. Bunyk *et al.*, Entanglement in a quantum annealing processor, Phys. Rev. X **4**, 021041 (2014).

[33] V. Choi, Minor-embedding in adiabatic quantum computation: I. The parameter setting problem, Quantum Inf. Process. **7**, 193 (2008).
[34] V. Choi, Minor-embedding in adiabatic quantum computation: II. Minor-universal graph design, Quantum Inf. Process. **10**, 343 (2011).
[35] N. Dattani, S. Szalay, and N. Chancellor, Pegasus: The second connectivity graph for large-scale quantum annealing hardware, arXiv:1901.07636.
[36] N. Dattani and N. Chancellor, Embedding quadratization gadgets on Chimera and Pegasus graphs, arXiv:1901.07676v1.
[37] R. Harris, J. Johansson, A. J. Berkley, M. W. Johnson, T. Lanting, S. Han, P. Bunyk, E. Ladizinsky, T. Oh, I. Perminov *et al.*, Experimental demonstration of a robust and scalable flux qubit, Phys. Rev. B **81**, 134510 (2010).
[38] A. Lucas, Ising formulations of many NP problems, Front. Phys. **2**, 5 (2014).
[39] F. Y. Wu, The Potts model, Rev. Mod. Phys. **54**, 235 (1982).
[40] D. Wang and R. Kleinberg, Analyzing quadratic unconstrained binary optimization problems via multicommodity flows, Discrete Appl. Math. **157**, 3746 (2009).
[41] K. L. Pudenz, T. Albash, and D. A. Lidar, Error-corrected quantum annealing with hundreds of qubits, Nat. Commun. **5**, 3243 (2014).
[42] T. Albash, V. Martin-Mayor, and I. Hen, Analog errors in Ising machines, Quantum Sci. Technol. **4**, 02LT03 (2019).
[43] M. Slutskii, T. Albash, L. Barash, and I. Hen, Analog nature of quantum adiabatic unstructured search, New J. Phys. **21**, 113025 (2019).
[44] V. Martin-Mayor and I. Hen, Unraveling quantum annealers using classical hardness, Sci. Rep. **5**, 15324 (2015).
[45] D. Venturelli, S. Mandrà, S. Knysh, B. O'Gorman, R. Biswas, and V. Smelyanskiy, Quantum Optimization of Fully Connected Spin Glasses, Phys. Rev. X **5**, 031040 (2015).
[46] Technical Description of the D-Wave Quantum Processing Unit, D-Wave User Manual 09-1109A-P, https://docs.dwavesys.com/docs/latest/_downloads/09-1109A-P_Technical_Description_of_DW_QPU.pdf.
[47] Z. Zhu, A. J. Ochoa, S. Schnabel, F. Hamze, and H. G. Katzgraber, Best-case performance of quantum annealers on native spin-glass benchmarks: How chaos can affect success probabilities, Phys. Rev. A **93**, 012317 (2016).
[48] In additional numerical simulations (not included in the present work), we have verified that normally distributed disorder leads to qualitatively identical conclusions as the one considered here.
[49] In the present work, we study only small systems, i.e., up to $NK = 16$ qubits. Effectively, this is the maximum number we can treat with numerical methods, i.e., exact diagonalization employed in this analysis.
[50] S. Santra, G. Quiroz, G. V. Steeg, and D. A. Lidar, Max 2-SAT with up to 108 qubits, New J. Phys. **16**, 045006 (2014).
[51] T. Graß, D. Raventós, B. Juliá-Díaz, C. Gogolin, and M. Lewenstein, Quantum annealing for the number-partitioning problem using a tunable spin glass of ions, Nat. Commun. **7**, 11524 (2016).
[52] H. Fehske, J. Schleede, G. Schubert, G. Wellein, V. S. Filinov, and A. R. Bishop, Numerical approaches to time evolution of complex quantum systems, Phys. Lett. A **373**, 2182 (2009).
[53] G. Torres-Vega, Chebyshev scheme for the propagation of quantum wave functions in phase space, J. Chem. Phys. **99**, 1824 (1993).
[54] C. Cook, H. Zhao, T. Sato, M. Hiromoto, and S. X.-D. Tan, GPU based parallel ising computing for combinatorial optimization problems in VLSI physical design, arXiv:1807.10750.
[55] Map coloring, Ocean Documentation, D-Wave Systems Inc., https://docs.ocean.dwavesys.com/en/latest/examples/map_coloring.html (retrieved 06/03/2018).
[56] E. D. Dahl, Programming with D-Wave: Map Coloring Problem D-Wave Systems Inc., https://www.dwavesys.com/sites/default/files/Map%20Coloring%20WP2.pdf (2013, retrieved 06/03/2018).
[57] Quantum programming: Map coloring example, https://vimeo.com/87188759 (2014, retrieved 06/03/2018).